

Preparation and characterization of B_xC_{1-x} thin films with the graphite structure

B. M. Way and J. R. Dahn

Department of Physics, Simon Fraser University, Burnaby, British Columbia, Canada V5A 1S6

T. Tiedje

Department of Physics and Electrical Engineering, University of British Columbia, Vancouver, British Columbia, Canada V6T 1Z1

K. Myrtle

Department of Physics, Simon Fraser University, Burnaby, British Columbia, Canada V5A 1S6

M. Kasrai

Department of Chemistry, University of Western Ontario, London, Ontario, Canada

(Received 23 January 1992)

Using chemical vapor deposition (CVD), we have prepared B_xC_{1-x} solid solutions for $0 < x < 0.17$, which have the graphite structure. By varying the relative proportions of benzene and boron trichloride in the CVD reactor, we are able to control the boron concentration in our thin-film samples. Grazing-incidence x-ray diffraction shows that for a series of films prepared at 900 °C, B_xC_{1-x} becomes more graphitic (with less turbostratic disorder) as x increases. There is a discontinuity between $x = 0.12$ and $x = 0.15$ in the variation of the distance between boron-carbon layers, as measured by the (002) plane spacing, which suggests the formation of an ordered BC_5 compound. Using synchrotron radiation, we measured the near-edge x-ray absorption of these films at the boron and carbon 1s edges as a function of the angle between the photon beam and the substrate. The dependence of the absorption with angle at both edges shows the same behavior as that reported for highly oriented pyrolytic graphite, where transitions to unoccupied π bands are suppressed when the photon beam is normal to the graphite layers, proving that the boron substitutionally replaces carbon in these materials.

INTRODUCTION

The preparation of boron-substituted graphite by the high-temperature reaction of B_4C and graphite was studied by Lowell,¹ who showed that the maximum amount of boron that could be substitutionally incorporated was 2.35% at 2350 °C. Recently, there have been reports²⁻⁵ of the preparation of graphite-structure boron-carbon, carbon-nitrogen, and boron-carbon-nitrogen hybrids using low-temperature (700 °C–1000 °C) chemical-vapor deposition (CVD). The boron-carbon materials were prepared from the reaction between benzene and BCl_3 in a horizontal "hot wall" CVD reactor. The prepared materials were characterized by a variety of techniques including x-ray and electron diffraction, Rutherford backscattering, electron-energy-loss spectroscopy, electrical resistivity, and by their ability to intercalate certain alkali metals. These results clearly show that graphite-structure B_xC_{1-x} materials with x as large as 0.25 can be prepared at 800 °C.

Boron-substituted graphite prepared by the methods of Lowell with less than 2.35% boron is currently marketed as "oxidation resistant" graphite. When subjected to heated air, carbon is oxidized to CO_2 and CO , which vaporize, but the boron becomes B_2O_3 , which is a stable solid. After sufficient exposure to heated air, the B_2O_3 layer that forms is sufficient to dramatically slow further reaction with heated air. It is possible that B_xC_{1-x} ma-

terials with $x > 0.0235$ will show much improved oxidation resistance.

The earlier studies of B_xC_{1-x} (Refs. 2–5) do not contain a systematic study of the variation of x as a function of the synthesis conditions. Therefore, there has not been an accurate study of the changes in the crystallography or physical properties of B_xC_{1-x} for a series of systematically prepared samples. B_xC_{1-x} materials may have applications and appear to have interesting properties,²⁻⁵ and so we decided to learn to synthesize them. Here we report the results of our syntheses and the subsequent characterization of the produced materials.

EXPERIMENT

Reagent grade benzene (Caledon Labs Ltd. ACS spectro-grade) and research grade BCl_3 (Matheson, 99.9%) were used as received. Ultra-high-purity argon (Linde, 99.999%) was used to flush the CVD reactor.

We used a Vacronic CVD-300-M system to make these films. The BCl_3 and the benzene are stored in a cylinder and a stainless-steel bottle, respectively, and are connected to Brooks 5850D mass-flow controllers via Teflon-lined stainless-steel hose. The output of the mass-flow controllers is fed directly to the reactor where the gases mix. Our reactor is pumped by a two-stage rotary pump isolated from the system by a liquid-nitrogen cold trap and a throttle valve. The throttle valve is controlled

by a pressure controller (MKS instruments) so that the pressure in the reactor can be set and maintained constant between 50 mTorr and 10 Torr. The reactor consists of a 75-mm-diam quartz tube within an electric furnace. No carrier gases were used in our depositions; boron trichloride and benzene each have sufficient vapor pressures at room temperature to be pumped through our flow controllers at sufficient rates when the reactor pressure is below 10 Torr. The flow rates for BCl_3 and benzene were calibrated. This was done by first evacuating the reactor at room temperature (volume = 4.3 liters), then measuring the time taken for the pressure to rise to 10 Torr under a particular flow setpoint with the pumping valve closed. Using the ideal-gas law, the flow rate is then simply determined.

We deposited films successfully on quartz slides, tantalum foil and copper foil. The results presented here are for films made on quartz at 900°C, which are similar to the films made on the other two substrates at the same temperature. A typical deposition consists of first loading the reactor with the substrates, followed by evacuation below 50 mTorr. The system is then continuously pumped while the reactor is heated to 900°C. Once the operating temperature has been attained and the pressure is below 50 mTorr, the BCl_3 and benzene flows are started and the system pressure is then maintained constant at 5 Torr. The flow rates were set at constant values between 6 and 20 cm^3/min at STP (SCCM) for benzene and between 0 and 80 SCCM for BCl_3 chosen to control the stoichiometry of the resulting film. The deposition continues for between 30 min and 1 h after which the reactive gas flows are stopped and the argon flow is started. The reactor is cooled below 100°C under argon flow before the films are removed. This procedure resulted in gray-black mirrorlike films for all the stoichiometries studied. The films adhere very well to the quartz-slide substrates. The film thicknesses varied somewhat with the stoichiometry of the gas mixture but were all near 1 μm . In each preparation, one $25 \times 25 \text{ mm}^2$ quartz slide and at least two $10 \times 10 \text{ mm}^2$ quartz slides were coated.

We used a Siemens D5000 diffractometer with a Cu x-ray tube operating in the Bragg-Brentano (flat plate sample) geometry for our initial measurements on the films. These measurements suffered through the appearance of large amounts of diffuse scattering from the quartz at scattering angles near the (002) peak of B_xC_{1-x} . To eliminate the signal from the quartz, we used a grazing incidence geometry and a detector equipped with long Soller slits to ensure the diffracted rays reaching the detector all scatter through twice the Bragg angle. In the grazing incidence geometry, the angle between the substrate and the incoming beam was set near the critical angle for total external reflection of the x rays from carbon, and the detector was scanned. This ensures that the x rays only penetrate about 100 Å which confines them to the film completely, removing all scattering from the quartz. For carbon, the critical angle is 0.217° for Cu $K\alpha$ radiation.⁶ Finally, we measured (002) and (004) rocking curves on samples that were relatively crystalline.

The stoichiometries of the samples were determined using a Perkin Elmer Physical Electronics Division model

595 scanning Auger microscope. The films were transferred to the vacuum chamber (1×10^{-9} Torr) and then sputtered using a 3-kV argon-ion beam for about 3 min to remove surface species. The boron and carbon *KLL* Auger electron intensities were measured and then the samples were further sputtered until Auger signals independent of sputter time were obtained. The composition of the surface of a sputtered film need not be the same as the bulk composition, so we also measured the Auger intensities for bulk B_4C powder (Johnson-Matthey) pressed into indium foil and sputtered under the same conditions as our film samples. When the Auger signals from the sputtered B_4C were corrected for the relative Auger sensitivities⁷ they give a stoichiometry of $\text{B}_{4.3}\text{C}$, suggesting that carbon and boron have almost the same sputter yield. The compositions of the films were determined by comparison to the Auger signals from B_4C , assuming it is stoichiometric. We estimate that the systematic error in our reported stoichiometries is less than 10%.

X-ray-absorption experiments were performed using the Canadian ERG beamline located at the Synchrotron Research Center of the University of Wisconsin. The details of the beamline have been described elsewhere.⁸ Our measurements were made using a total-electron-yield detector. The line from the center of the photon-beam spot on the sample to the center of the electron-yield detector makes an angle of 90° with respect to the incident photon direction. The sample could be rotated about an axis perpendicular to the plane containing the incident photon beam and the electron-yield detector, so that the angle of incidence of the photon beam with respect to the film could be controlled between 0° (normal incidence) and 70°. The instrumental resolution used here was about 0.2 eV at the boron 1s edge and about 0.4 eV at the carbon 1s edge.

To obtain reliable x-ray absorption spectroscopy (XAS) spectra of the carbon *K* edge, one must accurately measure the variation of the synchrotron beam intensity, I_0 , with photon energy because carbon contamination of the beamline optics leads to intensity variations in the region of interest. We made three independent measurements of the I_0 variation: (1) the current flow from a gold grid placed in the beam in front of the sample, (2) the absorption from a thick gold film deposited on Si, and (3) the absorption of a Si(100) wafer that had been freshly etched in HF prior to insertion into the vacuum chamber. The first measurement was made simultaneously with each of our measurements at the carbon edge, while the latter two were made independently. The data we show in this paper are the electron yield from the sample divided by the I_0 signal indicated by the absorption of the gold film. Using the other I_0 signals gave identical results.

RESULTS AND DISCUSSION

Figure 1 shows the atomic percent of boron in B_xC_{1-x} films deposited at 900°C as a function of the volume percentage of BCl_3 in the BCl_3 -benzene gas mixture. The most boron that we can incorporate in the films under these conditions is about 17%, close to the boron concen-

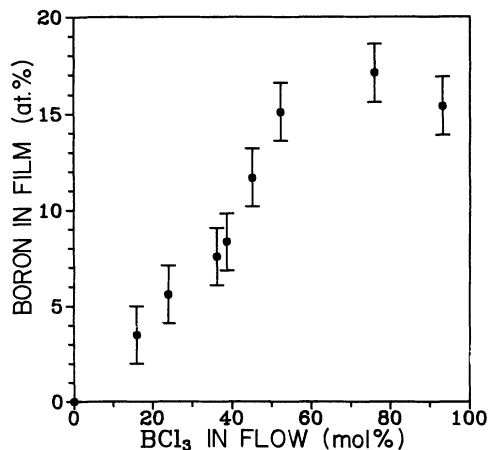


FIG. 1. Stoichiometry of B_xC_{1-x} films as a function of BCl_3 content in the BCl_3 -benzene gas mixture.

tration that would exist in BC_5 . In fact, the boron concentration seems to saturate once the gas mixture contains 50% BCl_3 . Shen *et al.*⁵ used a 2.5 molar excess of BCl_3 compared to benzene (71% by volume BCl_3 assuming molar volumes of 22.4 liters/mole for each) in their syntheses and claimed to make BC_3 at 900°C. They showed, however, that the maximum attainable boron concentration dropped rapidly with temperature, to 19.6% ($BC_{4.1}$) at 910°C and then to 15% ($BC_{5.6}$) at 1000°C. They did not, however, make any low-pressure (5 Torr) depositions like ours. We plan to study the effect of the deposition temperature on our films shortly.

Figure 2 shows the (002) Bragg peak of our B_xC_{1-x} films collected using the grazing incidence method. The

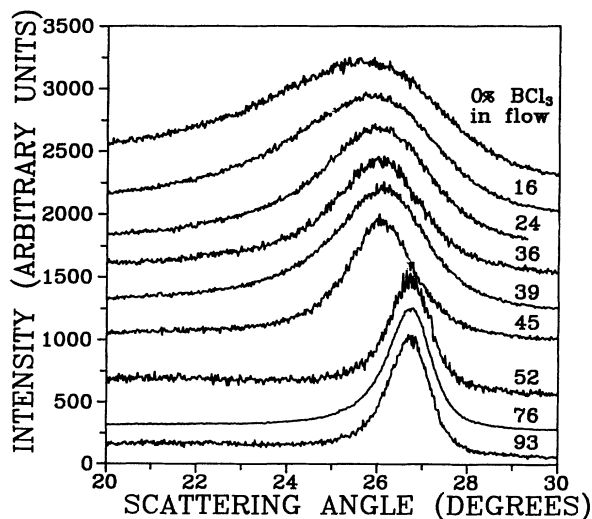


FIG. 2. Showing the (002) Bragg peak of B_xC_{1-x} samples made of 900°C. The numbers at the right, just above each data set, indicate the percentage of BCl_3 in the gas flow. The values of x can be obtained using Fig. 1. The data have been offset for clarity: from the bottom, the offsets are 0, 250, 500, 950, 1200, 1450, 1700, 1950, and 2200.

(002) peak moves to larger scattering angle (smaller plane spacing) and sharpens as the boron content of the films increases. The (002) spacing directly measures the distance between the boron-carbon layers analogous to the distance between carbon layers in pure graphite. The (002) peak motion seems to stop near 26.2° for the samples made with 36%, 39% and 45% BCl_3 in the flow, and then the (002) peak "jumps" to near 26.7° for the three higher-boron-content samples. We speculate that this may indicate the formation of a BC_5 phase having boron atoms arranged regularly within each layer; for lower boron concentrations, the boron is thought to be randomly substituting for carbon. Figure 3 shows the simplest possible arrangement for a single layer of ordered BC_5 . We have no information available to determine the stacking sequence of the layers, which will determine the registry of the boron superlattices in adjacent layers.

Figure 4(a) shows the variation of the spacing between the (002) planes, and Fig. 4(b) shows the full width at half maximum of the (002) peak both as a function of boron concentration in the film. Ruland⁹ reported the variation in (002) plane spacing and half-width for a series of carbons made by heating hydrocarbons to successively higher temperatures. As the carbon is heated more and more, the (002) spacing changes from about 3.45 Å at a treatment temperature of 1300°C to 3.35 Å, the (002) spacing of crystalline graphite, at a treatment temperature of 3000°C. Simultaneously, the (002) peak width sharpens as the "turbostratic" disorder⁹ between the graphitic layers diminishes and "graphitization" takes place. Turbostratic disorder is present in layered compounds with random rotations and translations between adjacent

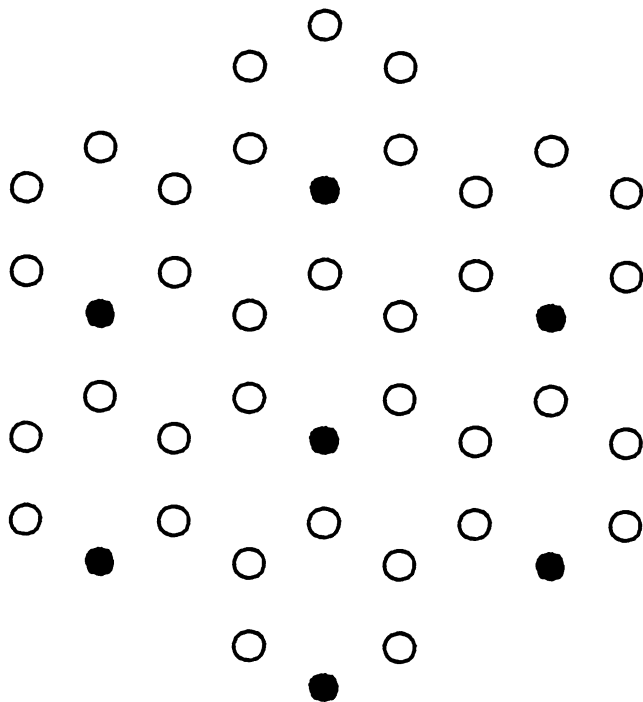


FIG. 3. Possible ordered arrangement for a single sheet of BC_5 . The open circles represent carbon atoms and the closed ones represent boron atoms.

layers, leading to fluctuations in the spacing between adjacent layers and hence to broadening of the (002) Bragg peak. As carbon graphitizes, the probability for such translations and rotations approaches zero, and all layers have the normal *ABABAB* registry. Partially graphitized carbons have some adjacent layers in the proper registry and some with random registry. Normally carbons do not begin graphitizing until above 1500 °C.⁹ Our results show that the addition of boron causes significant graphitization even at 900 °C, evidenced by the sharpening of the (002) peak as the boron concentration increases. Furthermore, for $B_{0.17}C_{0.83}$ we measure a (002) plane spacing of 3.336 Å, significantly smaller than for pure graphite [3.348 Å (Ref. 10)]. Lowell¹ showed that small additions of boron in crystalline graphite do cause a contraction in the *c* axis, in accord with our result. His data for the (002) spacing versus boron content give a slope of -0.00297 Å per percent boron. Using this value and the lattice constant for graphite, we extrapolate to 3.305 Å at 17% boron, significantly smaller than our measurements. We expect that some further contraction in the (002) plane spacing would occur if our $B_{0.17}C_{0.83}$ films could be made more crystalline. The contraction of the layer spacing with boron concentration is due to two effects: (1) an increase in structural ordering as graphitization occurs, and (2) a chemical bonding effect due to the smaller size of boron compared to carbon. It is difficult to separate the two effects.

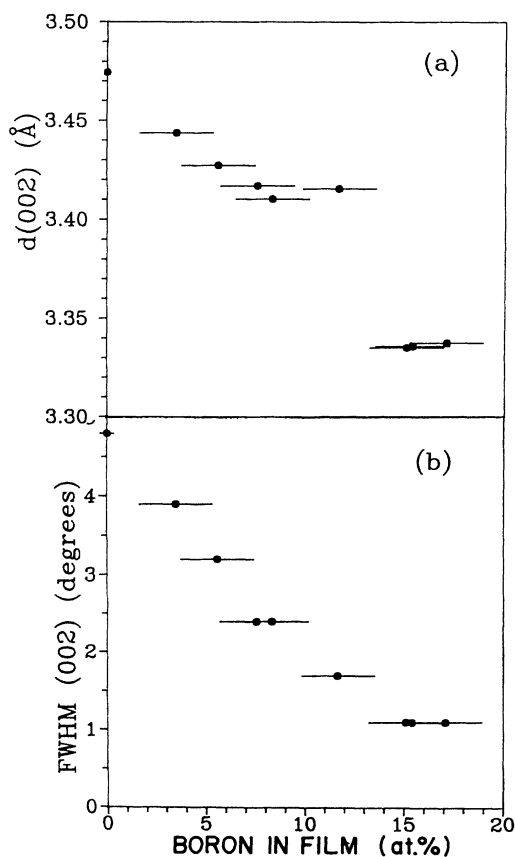


FIG. 4. (a) (002) layer spacing and (b) full width at half maximum of the (002) peak, as a function of x in B_xC_{1-x} .

Figures 5(a) and 5(b) show rocking curves collected on the (002) and (004) Bragg peaks of our film made with the highest concentration of BCl_3 in the gas flow. Rocking curves measure "mosaic spread," or the extent to which the layers are oriented parallel to the plane of the substrate. These data show that the majority of crystallites in the film are oriented with their *c* axes within $\pm 5^\circ$ of the normal to the substrate. This implies that only a small fraction of the crystallites are contributing to the (002) intensity measured in grazing incidence, where the normal to the layers must be tipped by about 13° to satisfy the Bragg condition. Rocking curves were only measured on the films with the highest boron concentrations. For those films with low boron concentrations, where the (002) peak is broad, the scattering from the quartz substrate is large compared with the (002) signal unless grazing incidence is used, making the rocking-curve measurement difficult.

Figure 6(a) shows the x-ray absorption at the carbon *K* edge measured at three angles of incidence for graphite powder (Johnson-Matthey) pressed onto copper tape. The pressing substantially orients the powder with the *c* axis normal to the tape. The data have been corrected for the I_0 variation as described above, and have been

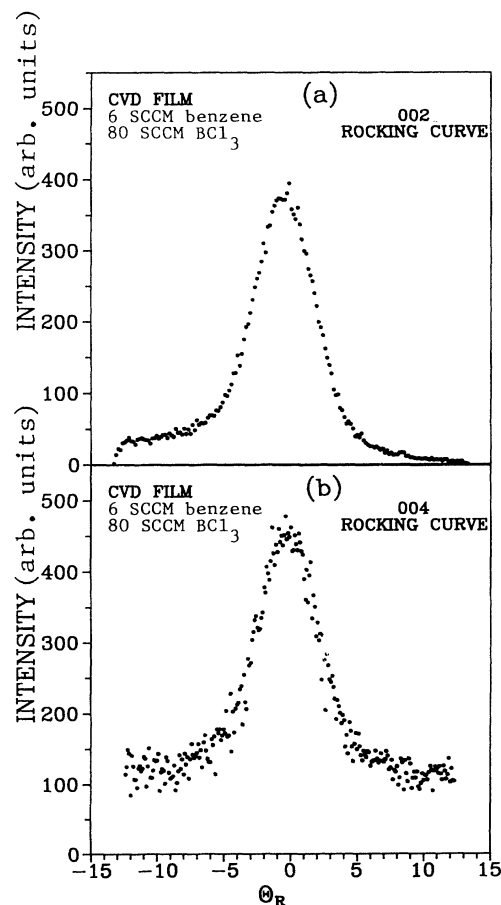


FIG. 5. Rocking curves for the (002) (a) and (004) (b) Bragg peaks of $B_{0.17}C_{0.83}$. The rocking angle θ_R is 0° when the angles of the incident and diffracted rays with respect to the normal to the substrate are the same.

scaled so that the absorption below the edge is the same. Figure 6(b) shows similar results for a CVD film prepared with only benzene in the reactor. The large peak near 285 eV is due to transitions from the carbon 1s state to unfilled π bands, and the large absorption commencing near 291 eV to transitions to unfilled σ bands.¹¹ Transitions to the π bands require that the electric field of the incoming photons have some component normal to the graphite layers, and, conversely, transitions to the σ bands require an electric field component parallel to the graphite layers.^{11,12} The angle dependence of the absorption reflects the strength of the electric-field components perpendicular and parallel to the sample surface, and shows that these two samples are predominantly aligned with their c axes normal to the substrate. There are some differences between the spectra of the two materials, particularly the broadening of the σ -band absorption and the appearance of a peak near 287 eV in the CVD film. A similar peak seen on other carbon films¹¹ has been attributed to "interlayer states." The results shown here suggest that these states are associated with turbostratic disorder, which is present in the CVD film but almost absent in the crystalline graphite powder.

Figures 7(a) and 7(b) show the carbon K edge for CVD

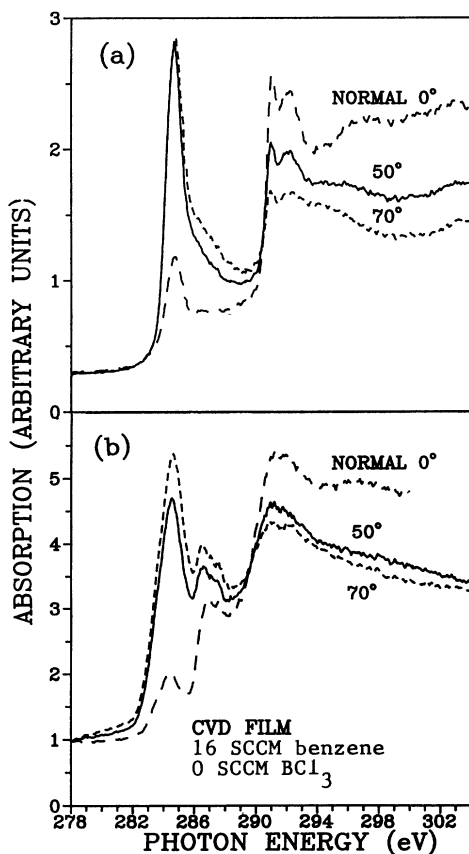


FIG. 6. Carbon 1s x-ray absorption for (a) oriented graphite powder and (b) a pure carbon film made by CVD. The data have been corrected for I_0 variations as described in the text. The angle of incidence of the photon beam with respect to the normal to the sample is indicated near each data set.

deposited $B_{0.05}C_{0.95}$ and $B_{0.17}C_{0.83}$, respectively. These data show the same general behavior as observed in Fig. 6, proving that the films are highly oriented. There is additional structure in the absorption right at the edge, evidenced by a shoulder (indicated by arrows in Fig. 7) at about 283 eV on the main π absorption. A similar shoulder, although weaker, has been previously observed¹³ for boron-doped carbon (with boron concentration less than 2.35%) made by the methods of Lowell.¹ This shoulder is caused by the empty π -bonding orbitals created by the incorporation of boron.

Figures 8(a) and 8(b) show measurements at the boron edge for the two samples described in Fig. 7. The dependence of the absorption with incidence angle is qualitatively similar to that at the carbon edge, proving that the boron 1s electron is transferred to final states with the same symmetry as those filled by an electron excited from the carbon 1s level. This shows that the boron atoms substitute for carbon in these B_xC_{1-x} films. Here the boron 1s electron is transferred to final states with predominantly π symmetry for photon energies between 184 and 192 eV, and to states with predominantly σ symmetry between 194 and 202 eV. The sharp peak in $B_{0.17}C_{0.83}$ near 193 eV has π character but we do not understand its origin. This sharp peak was only present in the film made with 93% BCl_3 in the gas flow. Since the boron concen-

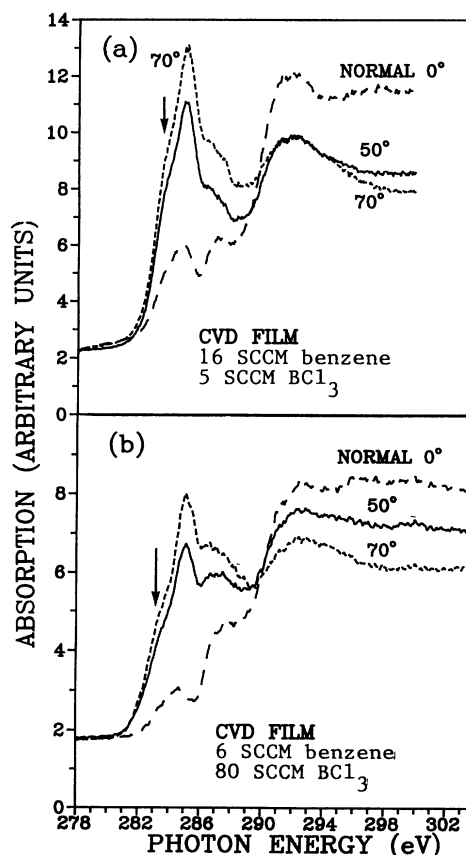


FIG. 7. Carbon 1s absorption for (a) $B_{0.05}C_{0.95}$ and (b) $B_{0.17}C_{0.83}$ films prepared by CVD. The arrows indicate empty π -bonding orbitals created by the incorporation of boron.

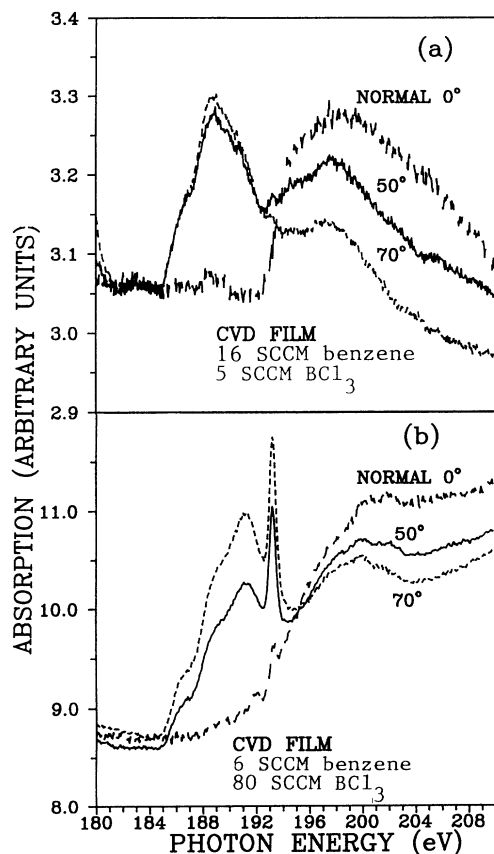


FIG. 8. Boron 1s absorption for (a) $B_{0.05}C_{0.95}$ and (b) $B_{0.17}C_{0.83}$ films prepared by CVD.

tration of the film saturates near 50% BCl_3 in the flow, it is possible that some boron-containing molecular impurity could be on the surface of the film giving rise to this sharp absorption. This molecule must be oriented with

its π orbitals perpendicular to the film to be consistent with the observed angle dependence of the absorption. The area of the sharp peak is small compared to the rest of the boron absorption, suggesting that if this peak is due to an impurity, the concentration is low. The details of the boron absorption will be the subject of further work. Furthermore, the strength of the boron absorption relative to the background scales as expected for these two films based on their stoichiometries, giving us further confidence in the compositions given in Fig. 1.

CONCLUSIONS

We have presented results that clearly show that a solid-solution series B_xC_{1-x} can be prepared for $0 \leq x \leq 0.17$ by CVD at $900^\circ C$. The value of x can be selected by controlling the relative amounts of benzene and BCl_3 in the gas flow. There is evidence for the formation of BC_5 , with boron atoms forming an ordered arrangement within each layer. The films become more highly graphitized as the boron concentration increases, and the spacing between (002) lattice planes in $B_{0.17}C_{0.83}$ is less than that in pure graphite. Rocking curves show that films with high boron concentration are oriented with their c axes normal to the substrate. The dependence of the x-ray absorption at the boron 1s edge with incidence angle is qualitatively the same as at the carbon 1s edge, proving that the boron in these materials has substituted for carbon.

ACKNOWLEDGMENTS

We thank the Natural Sciences and Engineering Research Council (NSERC) and The Simon Fraser University Presidents Fund for funding. One of us (B.M.W.) also thanks the NSERC for partial support. K. H. Tan provided essential assistance at the Wisconsin Synchrotron.

¹C. E. Lowell, *J. Am. Ceram. Soc.* **50**, 142 (1967).

²R. B. Kaner, J. Kouvetakis, C. E. Warble, M. E. Sattler, and N. Bartlett, *Mater. Res. Bull.* **22**, 399 (1987).

³J. Kouvetakis, T. Sasaki, C. Shen, R. Hagiwara, M. Lerner, K. M. Krishnan, and N. Bartlett, *Synth. Met.* **34**, 1 (1989).

⁴J. Kouvetakis, R. B. Kaner, M. L. Sattler, and N. Bartlett, *J. Chem. Soc. Chem. Commun.* **1986**, 1758.

⁵Byron C. Shen, Oliver K. Tse, J. Kouvetakis, K. M. Kirshnan, Kin-Man Yu, and N. Bartlett (unpublished).

⁶R. Friedenhan's, *Surf. Sci. Rep.* **10**, 105 (1989).

⁷L. E. Davis, N. C. MacDonald, P. W. Palmberg, G. E. Riach, and R. E. Weber, *Handbook of Auger Electron Spectroscopy*, 2nd ed. (Physical Electronics Division, Perkin Elmer Cor-

poration, Eden Prairie, MN, 1978).

⁸K. H. Tan, G. M. Bancroft, L. L. Coatsworth, and B. W. Yates, *Can. J. Phys.* **60**, 131 (1982).

⁹W. Ruland, *Acta Crystallogr.* **18**, 992 (1965).

¹⁰R. G. Wyckoff, *Crystal Structures*, 2nd ed. (Krieger, Malabar, FL, 1982), Vol. 1.

¹¹D. A. Fischer, R. M. Wentzcovitch, R. G. Carr, A. Contineza, and A. J. Freeman, *Phys. Rev. B* **44**, 1427 (1991).

¹²A. Zangwill, *Physics at Surfaces* (Cambridge University, New York, 1988).

¹³J. R. Dahn, J. N. Reimers, T. Tiedje, Y. Gao, A. K. Sleight, W. R. McKinnon, and S. Cramm, *Phys. Rev. Lett.* **68**, 835 (1992).